iScience, Volume *24*

Supplemental Information

Core Fermentation (CoFe) granules focus coordinated glycolytic mRNA localization and translation to fuel glucose fermentation

Fabian Morales-Polanco, Christian Bates, Jennifer Lui, Joseph Casson, Clara A. Solari, Mariavittoria Pizzinga, Gabriela Forte, Claire Griffin, Kirsten E.L. Garner, Harriet E. Burt, Hannah L. Dixon, Simon Hubbard, Paula Portela, and Mark P. Ashe

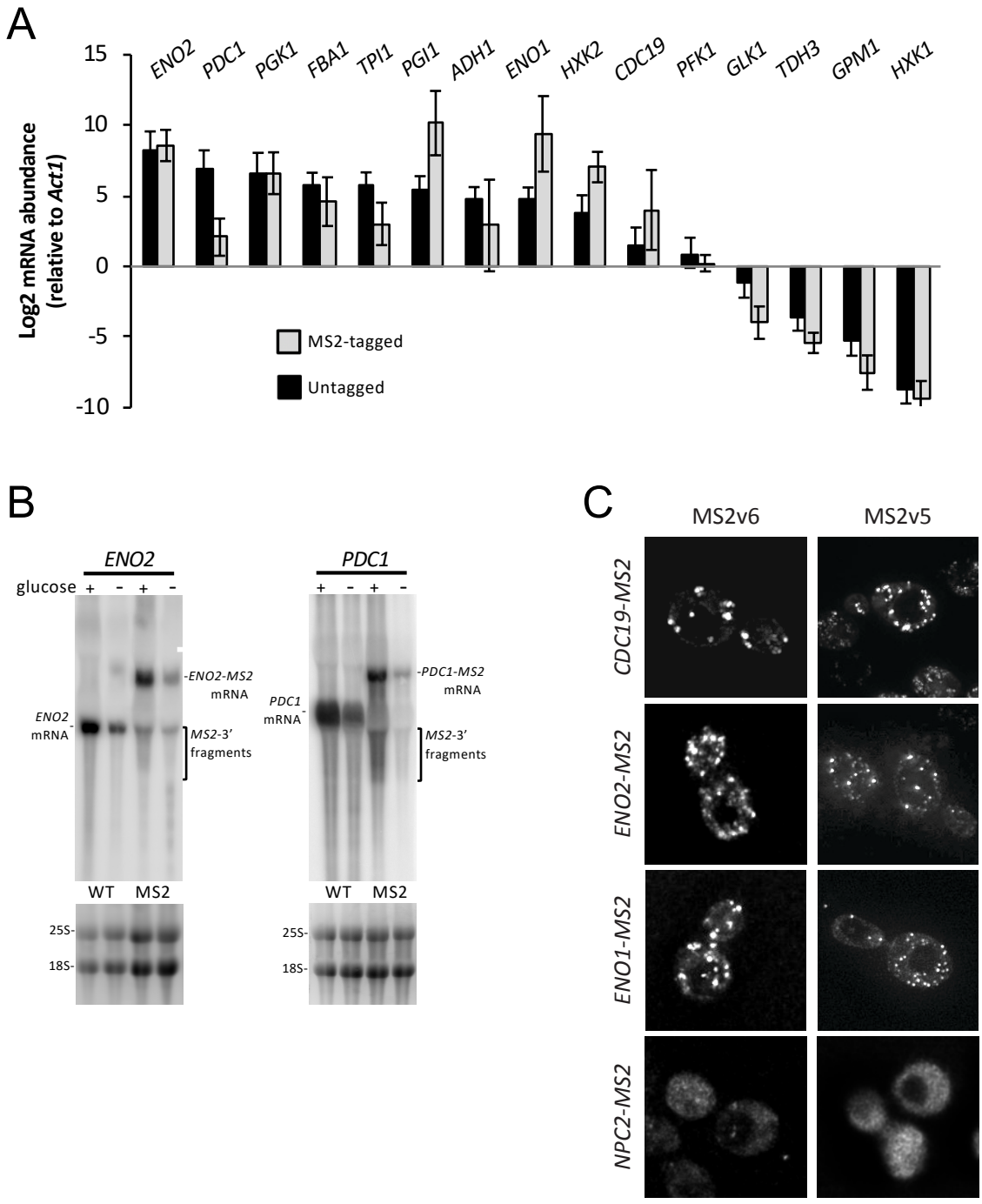

Figure S1. mRNA levels and the use of lower affinity MS2 stem loops support the premise that the glycolytic mRNAs are localized to RNA granules. Related to Figure 1. (A) Graph representing the relative fold change of *MS2*-tagged mRNAs relative to untagged mRNA levels. Error bars represent ± SE. (B) Northern blots of *ENO2* and *PDC1* mRNA in glucose replete and starved conditions in untagged strains or strains bearing the *MS2* tag. (C) *z*-stacked epifluorescent images of *CDC19, ENO1* and *ENO2* mRNAs tagged with both the MS2v6 and MS2v5 stem loop systems co-expressing the relevant MS2-CP-GFP fusion. MS2v5 images are the same as those shown in Figure 1. *ENO1* and *CDC19* MS2v6 constructs contain 24x stem loops, *ENO2* contains 12x stem loops. Scale bar: 2 μm

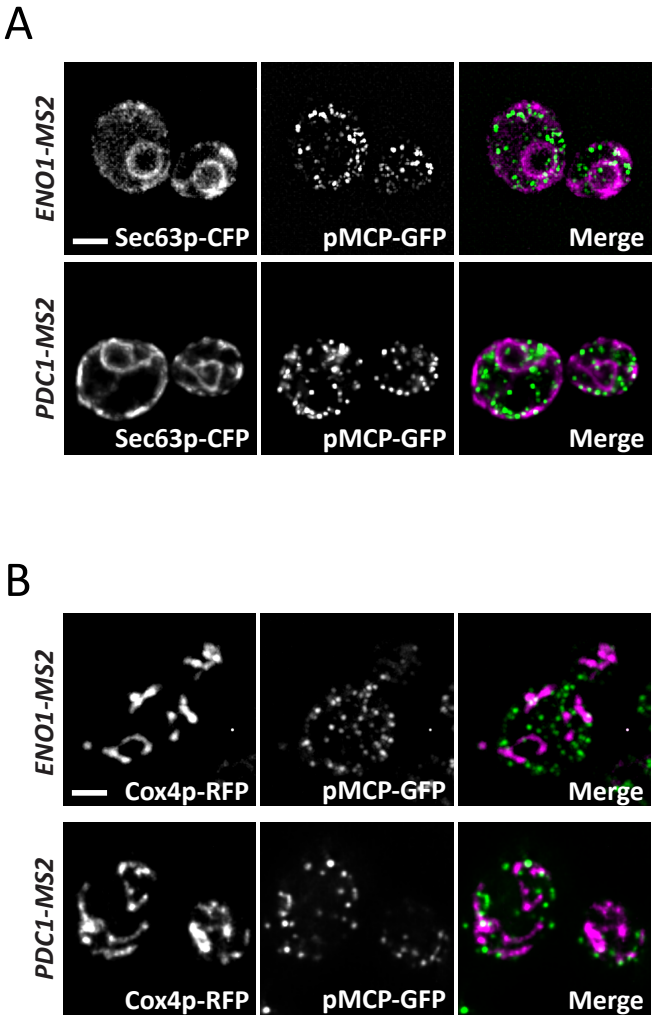

Figure S2. Glycolytic mRNA granules do not localize to ER or mitochondria. Related to Figures 3 and 4. z-stacked epifluorescent images of *ENO1* and *PDC1* mRNAs tagged with MS2 stem loops, visualized via co-expressed pMCP-GFP, with either an endoplasmic reticulum marker, Sec63p-CFP (A) or a mitochondrial marker, Cox4p-RFP, (B). Scale bars 2 μm.

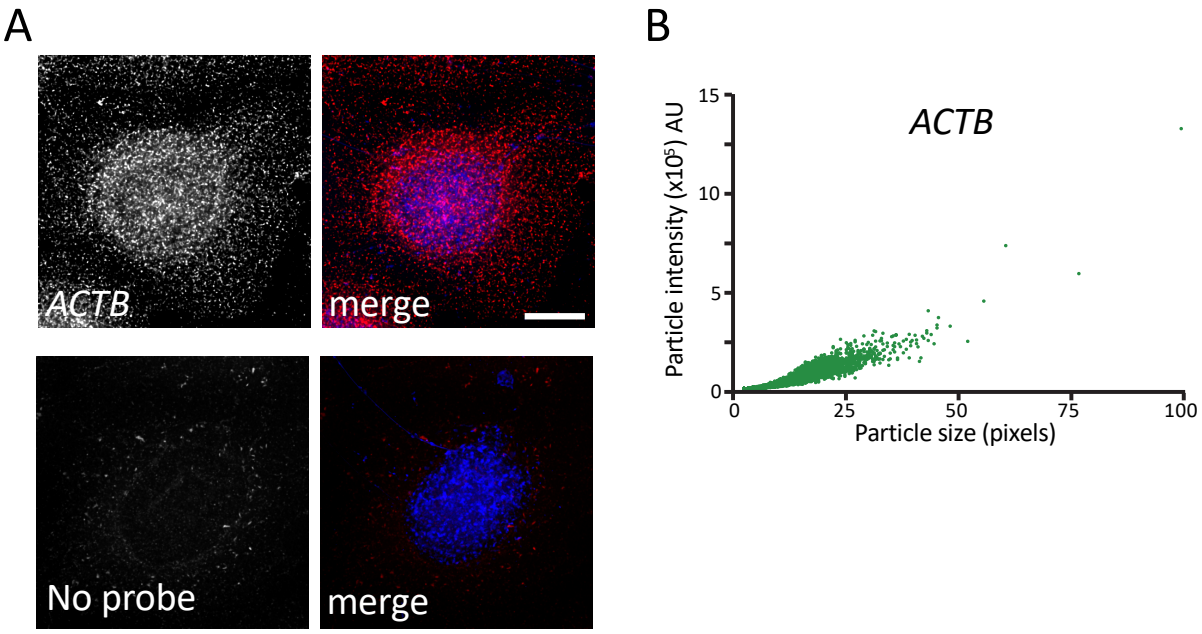

Figure S3. *ACTB* mRNA localizes diffusely throughout the cytoplasm. Related to Figure 7. (A) z-stacked epifluorescent images of HeLa cells. Cells were stained with DAPI and hybridized with either *ACTB* specific smFISH probes (top) or no probe as a control (bottom). Scale bar 10 μm. (B) Scatter plot of *ACTB* smFISH foci size and intensity, as detected by ComDet reveals very little evidence for large mRNA granules.

TRANSPARENT METHODS

EXPERIMENTAL MODEL AND SUBJECT DETAILS

Yeast growth conditions

Yeast experiments were performed in the *Saccharomyces cerevisiae* strain yMK467- a derivative of W303-1A (SCR_003093). Unless stated otherwise, experiments were performed after strains were grown in synthetic complete (SC) media with 2% glucose at 30°C to exponential phase. Strains used in this study are listed in Table I. For live-cell microscopy, cells were pelleted at 500xg for 3 minutes at 30°C, resuspended in pre-warmed (30°C) media lacking methionine and incubated for 30 min to induce expression of the pCP-GFP/mCh fusions prior to imaging. For growth on alternative carbon sources SC media was supplemented with 2% raffinose, 2% galactose or 3% ethanol. For stress conditions, cells were incubated in media lacking glucose for 10 minutes.

Human cell-line growth conditions

Human cell-line experiments were performed in HeLa cells (CVCL_0030), grown in Dulbecco's modified Eagle's medium supplemented with 10% fetal bovine serum at 37°C.

METHOD DETAILS

Yeast strain and plasmid construction

MS2 and PP7 tagged strains were generated as previously described (Haim-Vilmovsky and Gerst, 2011; Hocine et al., 2013; Tutucci et al., 2018), using plasmid reagents generously donated by Jeff Gerst and Robert Singer. Dual MS2 and PP7 tagged strains were generated by crossing the single tagged haploid strains. Subsequent diploid strains were selected, sporulated and the appropriate dual tagged haploid strains were verified by PCR. Expression of PP7 and MS2 coat protein-fluorescent protein fusions was driven from the inducible *MET25* promoter on plasmids that have been described previously (Haim-Vilmovsky and Gerst, 2011; Hocine et al., 2013; Tutucci et al., 2018; Lui et al., 2014). The strain harbouring a premature stop codon in the *PDC1* ORF was generated via recombination of a mutant PCR product generated from the *PDC1-MS2* tagged strain. More specifically, oligonucleotides with a specific mutation in the upstream primer were used to amplify a *PDC1::HIS5::MS2* cassette from genomic DNA prepared from an intermediate strain in the *PDC1-MS2* m-TAG procedure (Haim-Vilmovsky and Gerst, 2011). The mutation introduces a premature STOP codon in the *PDC1* ORF. The *PDC1::HIS5::MS2* cassette was then transformed and recombined into the *PDC1* locus of the yMK467 strain. Removal of the *HIS5* marker was carried out using a Cre recombinase strategy as previously described (Haim-Vilmovsky and Gerst, 2011). TRICK strains were generated using a similar approach to MS2 or

PP7 tagging, but using a DNA template developed for TRICK in yeast (Pizzinga et al., 2019). For generation of the yEPlac195-*PDC1* (p*PDC1-MS2*) plasmid, *PDC1-MS2* was amplified from genomic DNA of yMK1586 and cloned into the pGEM-T Easy vector and subsequently cloned into yEPLac195 using *Sph*I and *Sac*I restriction enzymes. A stem loop sequence (Vattem and Wek, 2004) was inserted upstream of the start codon in *PDC1* using Gibson assembly (Gibson et al., 2009) to generate plasmid yEPlac195-PDC1-SL (p*PDC1*-MS2 (sl)).

Single molecule fluorescent *in situ* hybridisation (smFISH)

For yeast cultures, smFISH was performed as previously described (Pizzinga et al., 2019). In brief, exponential-phase yeast were fixed in 4% EM-grade formaldehyde (15714-S; Electron Microscopy Sciences) for 45 min, then spheroplasted and permeablized with 70% ethanol. Gene-specific 20nt antisense oligonucleotides were designed with a 59nt Flap sequence, to which fluorescently labelled oligonucleotides were annealed (Pizzinga et al., 2019; Tsanov et al., 2016). The conjugated fluorophores included Alexa Fluor 488, Alexa Fluor 546, ATTO 590 and Alexa Fluor 648. After careful titration of the probe, 20 pmol fluorescently labelled smFISH probe was found to generate optimal signal relative to background when added to the cells in hybridization buffer (10 mg E. coli tRNA, 2 mM Ribonucleoside Vanadyl Complex, 200 µg/ml BSA, 10% dextran sulfate, 10% formamide, and 2× SSC in nuclease-free water). This hybridization buffer – probe mix was then added to cells and incubated overnight at 37°C, with gentle agitation. Cells were then washed in 10% formamide and 2× SSC and adhered to 0.01% poly-L-lysine–coated coverslips before mounting in ProLong diamond antifade mounting solution with DAPI (Life Technologies Cat# P36970).

For human cell experiments, HeLa cells were seeded in Dulbecco's modified Eagle's medium supplemented with 10% fetal bovine serum onto 13 mm laminin coated coverslips in sterile 24-well plates, then were fixed in methanol for 10 min at -20^{o}C. Fixed cells were washed in 10% Formamide, 2x SSC buffer in nuclease-free water for 30 min at room temperature, then hybridized probes (as above) were added at a concentration of 25 nM for Cy7-conjugated probes and 75 nM for Cy5-conjugated probes at 37^{o}C overnight. Cells were then washed and mounted (Tsanov et al., 2016). An extensive series of experiments was undertaken to optimise the probe concentration and fixation method such that the no signal was detected in the various channels when a particular probe was absent.

Live-cell fluorescent microscopy

All yeast live-cell epifluorescent microscopy was performed on a Nikon Eclipse E600 or a Delta Vision microscope (Applied Precision) equipped with a Coolsnap HQ camera (Photometrics),

using a 100x/ 1.40 NA oil plan Apo objective. Fluorescent parameters for each fluorophore are as follows; GFP (excitation-490/20 nm, emission- 535/50 nm); mCherry (excitation- 572/35 nm, emission-632/60 nm); and CFP (excitation- 436/10 nm, emission- 465/30). For routine live-cell imaging, exponentially growing cells were viewed on poly-L-lysine coated glass slides and images were taken with a *z*-spacing of 0.2µm. Images were acquired using Softworx 1.1 (Applied Precision), or Metamporph (Molecular Devices) software and processed using Image J software package (National Institute of Health, NIH).

Fixed-cell fluorescent microscopy

Images of human cells were acquired on an Olympus IX83 inverted microscope using Lumencor LED excitation, a *100x* objective and the Penta filter set. The images were collected using a *Retiga R6 (Qimaging)* CCD camera with a *z*-optical spacing of 0.2 µm. Raw images were then deconvolved using the Huygens Professional software (Scientific Volume Imaging).

Yeast smFISH images were collected on a Leica TCS SP8 AOBS inverted gSTED microscope using a 100x/1.40 Plan APO objective and 1x confocal zoom, as described previously (Pizzinga et al., 2019). DAPI staining was detected using a photon multiplying tube with a blue diode 405nm laser (5%). Confocal images of smFISH signals were collected using hybrid detectors with the following detection mirror settings; Alexa Fluor 488 498-536nm; Alexa Fluor 546 556-637nm (5 to 35µs gating); ATTO 590 603-637nm; Alexa Fluor 647 657-765nm using the 488nm (60%), 550nm (60%), 593nm (60%) and 646nm (60%) excitation laser lines, respectively. Images were collected sequentially in 200nm *z*-sections. Acquired images were subsequently deconvolved and background subtracted using Huygens Professional (Scientific Volume Imaging).

Quantitative RT-PCR (qRT-PCR)

RNA preparations were carried out using Trizol as described by the manufacturer (Thermofisher scientific, Cat#15596026), followed by isopropanol precipitation then treatment with Turbo DNase (Thermofisher scientific, Cat#AM2238). qRT-PCR was performed in a two-step manner using a ProtoScript First Strand cDNA synthesis kit (New England Biolabs, Cat#E6300S) and iQ SYBR Green Supermix (Bio-Rad, Cat#1708880) according to manufacturer's instructions. Reactions were performed using 100ng of cDNA. iTaq Universal SYBR Green One Step Kit (Bio-Rad, Cat#1725150) was used to carry out one-step qRT-PCR and reactions were performed using 300ng of RNA. A CFx Connect Real-Time system was used to run reactions. Samples were run in triplicate and normalized to *ACT1* mRNA, and the fold change was calculated using either the $2^{-\Delta\Delta Cq}$ or the Pfaffl method (Livak and Schmittgen, 2001; Pfaffl, 2001).

QUANTIFICATION AND STATISTICAL ANALYSIS

Quantification of microscopy and statistics.

For quantification of granule numbers per cell from live cell experiments, 50 cells were counted for each strain. For quantification of overlapping MS2 and PP7 signal in double-tagged strains or TRICK strains, 100 granules were considered for each strain over three biological repeats. GraphPad Prism 6 (GraphPad Software, Inc.) was used to produce the graphs and to calculate the standard deviation, indicated by error bars. Two-way ANOVA was performed using GraphPad Prism 6. * denotes a P value < 0.0001.

Yeast smFISH images were processed and analysed using FISH-quant (Mueller et al., 2013) and FindFoci (Herbert et al., 2014) to identify spot position and size and provide spot enhancement via dual Gaussian filtering. To account for differences in smFISH signal intensity between fluorophores and experiments, different intensity thresholds for each channel/image were determined manually. However, the same thresholds were applied to all cells in that image. Cell outlines were automatically generated using a modified version of the CellProfiler (Carpenter et al., 2006) pipeline provided with FISH-quant that utilizes background cytoplasmic DAPI staining rather than brightfield images to determine cytoplasmic cell boundaries. Spot colocalization and other foci characteristics were assessed and quantified using custom scripts in python to scrape data from FISHquant into long format and R for more detailed analysis. Human cell line smFISH images were analyzed using the Image J ComDet plugin, which generates values for particle size (area) in pixels where each pixel = 45x45 nm and particle intensity in arbitrary units.

Colocalization analysis in yeast cells was performed by pairing spots between channels based on spot centroid distance in 3D space (Eliscovich et al., 2017). Spots were deemed to colocalize if the 3D distance between centroids was less than the radius of either of the two spots, i.e. if the centroid of one spot existed within the radius of another spot. mRNA quantitation was performed using Gaussian fitting, as described previously (Pizzinga et al., 2019). To account for stochasticity in initial fitting parameters, this fitting was repeated 1,000 times and averaged. Simulated controls were based on the Monte Carlo simulation method (Fletcher et al., 2010). Real spots identified using smFISH sampled using varying spot characteristics, such as size in x, y and z, and these were arbitrarily positioned within a simulated volume typical of a yeast cell as measured using the custom CellProfiler pipeline. This volume includes RNA depleted regions of the cell such as the vacuole. A variable number of spots were selected for the simulation of each mRNA dependent upon the average number of foci observed per cell for that particular mRNA. The colocalization of these randomly positioned foci was subsequently processed using the same script outlined above, and iterated 1,000 times per pairwise comparison. For the human cell line

colocalisation analysis, the ComDet plugin was used on ImageJ which takes a similar centroid-centroid overlap approach to that described above (Katrukha 2020).

KEY RESOURCES TABLE

REAGENT or RESOURCE	SOURCE	IDENTIFIER
Chemicals, Peptides, and Recombinant Proteins		
EM-grade formaldehyde	Electron Microscopy Sciences	Cat#15714-S
ProLong Diamond Antifade Mountant	Life Technologies	Cat#P36970
Critical Commercial Assays		
Turbo DNase	Thermofisher Scientific	Cat#15596026
ProtoScript First Strand cDNA synthesis kit	New England Biolabs	Cat#E6300S
iQ SYBR Green Supermix	Bio-Rad	Cat#1708880
iTaq Universal SYBR Green One Step Kit	Bio-Rad	Cat#1725150
Stellaris® FISH Probes, Human ACTB with Quasar® 570 Dye	Biosearch Technologies	Cat#VSMF-2002-5
Experimental Models: Organisms/Strains		
yMK467 *MATα ADE2 his3-11,15 leu2-3,112 trp1-1 ura3-1*	(Campbell et al., 2005)	
yMK807 MATa ADE2 his3-11,15 leu2-3,112 trp1-1 ura3-1	(Campbell et al., 2005)	
yMK1577 *MATα ADE2 his3-11,15 leu2-3,112 trp1-1 ura3-1 ENO2-MS2L p[MS2-GFP$_3$ HIS3]*	(Lui et al., 2014)	
yMK1586 *MATα ADE2 his3-11,15 leu2-3,112 trp1-1 ura3-1 PDC1-MS2L p[MS2-GFP$_3$ HIS3]*	(Lui et al., 2014)	
yMK1651 *MATα ADE2 his3-11,15 leu2-3,112 trp1-1 ura3-1 PDC1-MS2L DCP2-CFP p[MS2-GFP$_3$ HIS3]*	(Lui et al., 2014)	
yMK2257 *MATα ADE2 his3-11,15 leu2-3,112 trp1-1 ura3-1 ENO2-PP7L PDC1-MS2L p[MS2-mCh$_3$ HIS3] p[PP7-GFP$_2$ URA3]*	(Lui et al., 2014)	
yMK2412 *MATα ADE2 his3-11,15 leu2-3,112 trp1-1 ura3-1 PFK1-MS2L p[MS2-GFP$_3$ HIS3]*	This Study	NA
yMK2413 *MATα ADE2 his3-11,15 leu2-3,112 trp1-1 ura3-1 PYK2-MS2L p[MS2- GFP$_3$ HIS3]*	This Study	NA
yMK2415 *MATα ADE2 his3-11,15 leu2-3,112 trp1-1 ura3-1 PFK2-MS2L (5 loops) p[MS2- GFP$_3$ HIS3]*	This Study	NA
yMK2416 *MATα ADE2 his3-11,15 leu2-3,112 trp1-1 ura3-1 FBA1-MS2L p[MS2- GFP$_3$ HIS3]*	This Study	NA
yMK2429 *MATα ADE2 his3-11,15 leu2-3,112 trp1-1 ura3-1*	This Study	NA
yMK2430 *MATα ADE2 his3-11,15 leu2-3,112 trp1-1 ura3-1 TPI1-MS2L p[MS2-GFP$_3$ HIS3]*	This Study	NA
yMK2431 *MATα ADE2 his3-11,15 leu2-3,112 trp1-1 ura3-1 GLK1-MS2L p[MS2-GFP$_3$ HIS3]*	This Study	NA
yMK2447 *MATα ADE2 his3-11,15 leu2-3,112 trp1-1 ura3-1 ADH1-MS2L p[MS2-GFP$_3$ HIS3]*	This Study	NA
yMK2452 *MATα ADE2 his3-11,15 leu2-3,112 trp1-1 ura3-1 PDC1-MS2L (sc) DCP2-CFP p[MS2-GFP$_3$ HIS3]*	This Study	NA
yMK2480 *MATα ADE2 his3-11,15 leu2-3,112 trp1-1 ura3-1 PFK2-MS2L p[MS2-GFP$_3$ HIS3]*	This Study	NA
yMK2535 *MATα ADE2 his3-11,15 leu2-3,112 trp1-1 ura3-1 PGK1-MS2L p[MS2- GFP$_3$ HIS3]*	This Study	NA
yMK2468 *MATα ADE2 his3-11,15 leu2-3,112 trp1-1 ura3-1 ENO1-MS2L p[MS2- GFP$_3$ HIS3]*	This Study	NA
yMK580 *MATα ADE2 his3-11,15 leu2-3,112 trp1-1 ura3-1 HXK1-MS2L p[MS2- GFP$_3$ HIS3]*	This Study	NA
yMK2582 *MATα ADE2 his3-11,15 leu2-3,112 trp1-1 ura3-1 CDC19-MS2L p[MS2- GFP3 HIS3]*	This Study	NA

yMK2585 *MATα ADE2 his3-11,15 leu2-3,112 trp1-1 ura3-1 TDH3-MS2L p[MS2- GFP$_3$ HIS3]*	This Study	NA
yMK2588 *MATα ADE2 his3-11,15 leu2-3,112 trp1-1 ura3-1 GLO1-MS2L p[MS2- GFP$_3$ HIS3]*	This Study	NA
yMK2594 *MATα ADE2 his3-11,15 leu2-3,112 trp1-1 ura3-1 ENO2-PP7L PFK1-MS2L p[MS2-mCh$_3$ HIS3] p[PP7–GFP$_2$ URA3]*	This Study	NA
S. cerevisiae: yMK2596 *MATα ADE2 his3-11,15 leu2-3,112 trp1-1 ura3-1 ENO2-PP7L PGI1-MS2L p[MS2-mCh$_3$ HIS3] p[PP7–GFP$_2$ URA3]*	This Study	NA
yMK2600 *MATα ADE2 his3-11,15 leu2-3,112 trp1-1 ura3-1 ENO2-PP7L ADH1-MS2L p[MS2-mCh$_3$ HIS3] p[PP7–GFP$_2$ URA3]*	This Study	NA
yMK2601 *MATα ADE2 his3-11,15 leu2-3,112 trp1-1 ura3-1 ENO2-PP7L CDC19-MS2L p[MS2-mCh$_3$ HIS3] p[PP7–GFP$_2$ URA3]*	This Study	NA
yMK2602 *MATα ADE2 his3-11,15 leu2-3,112 trp1-1 ura3-1 ENO2-PP7L TDH3-MS2L p[MS2-mCh$_3$ HIS3] p[PP7–GFP$_2$ URA3]*	This Study	NA
yMK2603 *MATα ADE2 his3-11,15 leu2-3,112 trp1-1 ura3-1 ENO2-PP7L PFK2-MS2L p[MS2-mCh$_3$ HIS3] p[PP7–GFP$_2$ URA3]*	This Study	NA
yMK2604 *MATα ADE2 his3-11,15 leu2-3,112 trp1-1 ura3-1 ENO2-PP7L TPI1-MS2L p[MS2-mCh$_3$ HIS3] p[PP7–GFP$_2$ URA3]*	This Study	NA
yMK2699 *MATα ADE2 his3-11,15 leu2-3,112 trp1-1 ura3-1 HXK2-MS2L p[MS2- GFP$_3$ HIS3]*	This Study	NA
yMK2700 *MATα ADE2 his3-11,15 leu2-3,112 trp1-1 ura3-1 PFK26-MS2L p[MS2- GFP$_3$ HIS3]*	This Study	NA
yMK2705 *MATα ADE2 his3-11,15 leu2-3,112 trp1-1 ura3-1 ENO2-PP7L GPM1-MS2L p[MS2 -mCh$_3$ HIS3] p[PP7 –GFP$_2$ URA3]*	This Study	NA
yMK2738 *MATα ADE2 his3-11,15 leu2-3,112 trp1-1 ura3-1 DCP2-CFP p[MS2- GFP$_3$ HIS3] p[PDC1-MS2-SL]*	This Study	NA
yMK3162 *MATα ADE2 his3-11,15 leu2-3,112 trp1-1 ura3-1 DCP2-CFP p[MS2- GFP$_3$ HIS3] p[PDC1-MS2]*	This Study	NA
yMK3176 *MATα ADE2 his3-11,15 leu2-3,112 trp1-1 ura3-1 GPM1-MS2L p[MS2- GFP$_3$ HIS3]*	This Study	NA
yMK3397 *MATα ADE2 his3-11,15 leu2-3,112 trp1-1 ura3-1 PGI1-MS2L p[MS2- GFP3 HIS3]*	This Study	NA
yMK5000 *MATα ADE2 his3-11,15 leu2-3,112 trp1-1 ura3-1 ENO1-MS2v6L p[MS2- GFP2 LEU2]*	This Study	NA
yMK5001 *MATα ADE2 his3-11,15 leu2-3,112 trp1-1 ura3-1 ENO2-MS2v6L p[MS2- GFP2 LEU2]*	This Study	NA
yMK5002 *MATα ADE2 his3-11,15 leu2-3,112 trp1-1 ura3-1 CDC19-MS2v6L p[MS2- GFP2 LEU2]*	This Study	NA
yMK5003*MATα ADE2 his3-11,15 leu2-3,112 trp1-1 ura3-1 NPC2-MS2v6L p[MS2- GFP2 LEU2]*	This Study	NA
yMK3471 *MATα ADE2 his3-11,15 leu2-3,112 trp1-1 ura3-1 PDC1-MS2L SEC63-CFP p[MS2-GFP$_3$ HIS3]*	This Study	NA
yMK3472 *MATα ADE2 his3-11,15 leu2-3,112 trp1-1 ura3-1 ENO1-MS2L SEC63-CFP p[MS2-GFP$_3$ HIS3]*	This Study	NA
yMK3473 *MATα ADE2 his3-11,15 leu2-3,112 trp1-1 ura3-1 PDC1-MS2L p[MS2-GFP$_3$ HIS3] p[COX4-RFP URA3]*	This Study	NA
yMK3474 *MATα ADE2 his3-11,15 leu2-3,112 trp1-1 ura3-1 ENO1-MS2L p[MS2-GFP$_3$ HIS3] p[COX4-RFP URA3]*	This Study	NA
Oligonucleotides		
X-Flap Alexa Fluor 546: 5'Alex546N-CACTGAGTCCAGCTCGAAACTTAGGAGG -3'AlexF546N	Integrated DNA Technologies	NA
Y-Flap Alexa Fluor 488: 5'Alex488N-AATGCATGTCGACGAGGTCCGAGTGTAA-	Integrated DNA Technologies	NA

3'AlexF488N		
Z-Flap Alexa Fluor 647: 5'Alex647N-CTTATAGGGCATGGATGCTAGAAGCTGG-3'AlexF647N	Integrated DNA Technologies	NA
Y-Flap ATTO 590: 5'ATTO590N-AATGCATGTCGACGAGGTCCGAGTGTAA-3'ATTO590N	Integrated DNA Technologies	NA
X-Flap ATTO 590: 5'ATTO590N-CACTGAGTCCAGCTCGAAACTTAGGAGG -3'ATTO590N	Integrated DNA Technologies	NA
Z-Flap ATTO 590: 5'ATTO590N-CTTATAGGGCATGGATGCTAGAAGCTGG -3'ATTO590N	Integrated DNA Technologies	NA
Recombinant DNA		
yEPLac195-PDC1	This Study	NA
yEPLac195-PDC1-SL	This Study	NA
pMCP-GFP	(Haim-Vilmovsky et al., 2011)	pMS2-CP-GFP(x3)
12xMS2v5	(Haim-Vilmovsky et al., 2011)	pLOXHIS5MS2L
pMCP-mCh	(Lui et al., 2014)	NA
pPP7CP-GFP	(Hocine et al., 2013)	Addgene Plasmid #45931
24xPP7SL	(Hocine et al., 2013)	Addgene Plasmid #45163
12xMS2v6-loxP	(Tutucci et al., 2018)	Addgene Plasmid #104392
24xMS2v6-loxP	(Tutucci et al., 2018)	Addgene Plasmid #104393
MCPv6-NLS	(Tutucci et al., 2018)	Addgene Plasmid #104394
Software and Algorithms		
Softworx v1.1	Applied Precision	http://www.cytivalifesciences.com
Metamorph	Molecular Devices	https://www.moleculardevices.com/products/cellular-imaging-systems/acquisition-and-analysis-software/metamorph-microscopy#Overview
FISHQuant	(Mueller et al., 2013)	https://bitbucket.org/muellerflorian/fish_quant
FindFoci	(Herbert et al., 2014)	http://www.sussex.ac.uk/gdsc/intranet/microscopy/UserSupport/AnalysisProtocol/imagej/findfoci
CellProfiler 3.0	(Carpenter et al., 2006)	https://cellprofiler.org/
Prism 6	GraphPad	https://www.graphpad.com/scientific-software/prism/

Huygens Professional	Scientific Volume Imaging	https://svi.nl/HomePage

Supplementary References

Campbell, S.G., Hoyle, N.P., and Ashe, M.P. (2005). Dynamic cycling of eIF2 through a large eIF2B-containing cytoplasmic body: implications for translation control. J Cell Biol *170*, 925-934.

Carpenter, A.E., Jones, T.R., Lamprecht, M.R., Clarke, C., Kang, I.H., Friman, O., Guertin, D.A., Chang, J.H., Lindquist, R.A., Moffat, J.*, et al.* (2006). CellProfiler: image analysis software for identifying and quantifying cell phenotypes. Genome Biol *7*, R100.

Eliscovich, C., Shenoy, S.M., and Singer, R.H. (2017). Imaging mRNA and protein interactions within neurons. Proc Natl Acad Sci USA *114*, E1875-E1884.

Fletcher, P.A., Scriven, D.R., Schulson, M.N., and Moore, E.D. (2010). Multi-image colocalization and its statistical significance. Biophys J *99*, 1996-2005.

Gibson, D.G., Young, L., Chuang, R.Y., Venter, J.C., Hutchison, C.A., 3rd, and Smith, H.O. (2009). Enzymatic assembly of DNA molecules up to several hundred kilobases. Nat methods *6*, 343-345.

Haim-Vilmovsky, L., and Gerst, J.E. (2011). Visualizing endogenous mRNAs in living yeast using m-TAG, a PCR-based RNA aptamer integration method, and fluorescence microscopy. Methods Mol Biol *714*, 237-247.

Haim-Vilmovsky, L., Gadir, N., Herbst, R.H., and Gerst, J.E. (2011). A genomic integration method for the simultaneous visualization of endogenous mRNAs and their translation products in living yeast. RNA *17*, 2249-2255.

Herbert, A.D., Carr, A.M., and Hoffmann, E. (2014). FindFoci: a focus detection algorithm with automated parameter training that closely matches human assignments, reduces human inconsistencies and increases speed of analysis. PLoS One *9*, e114749.

Hocine, S., Raymond, P., Zenklusen, D., Chao, J.A., and Singer, R.H. (2013). Single-molecule analysis of gene expression using two-color RNA labeling in live yeast. Nat methods *10*, 119-121.

Katrukha E. 2020, ComDet plugin for ImageJ, v0.5.3, Zenodo, doi:10.5281/zenodo.4281064

Livak, K.J., and Schmittgen, T.D. (2001). Analysis of relative gene expression data using real-time quantitative PCR and the 2(-Delta Delta C(T)) Method. Methods *25*, 402-408.

Lui, J., Castelli, L.M., Pizzinga, M., Simpson, C.E., Hoyle, N.P., Bailey, K.L., Campbell, S.G., and Ashe, M.P. (2014). Granules harboring translationally active mRNAs provide a platform for P-body formation following stress. Cell Rep *9*, 944-954.

Mueller, F., Senecal, A., Tantale, K., Marie-Nelly, H., Ly, N., Collin, O., Basyuk, E., Bertrand, E., Darzacq, X., and Zimmer, C. (2013). FISH-quant: automatic counting of transcripts in 3D FISH images. Nat Methods *10*, 277-278.

Pfaffl, M.W. (2001). A new mathematical model for relative quantification in real-time RT-PCR. Nucleic Acids Res 29, e45.

Pizzinga, M., Bates, C., Lui, J., Forte, G., Morales-Polanco, F., Linney, E., Knotkova, B., Wilson, B., Solari, C.A., Berchowitz, L.E.*, et al.* (2019). Translation factor mRNA granules direct protein synthetic capacity to regions of polarized growth. J Cell Biol *218*, 1564-1581.

Tsanov, N., Samacoits, A., Chouaib, R., Traboulsi, A.M., Gostan, T., Weber, C., Zimmer, C., Zibara, K., Walter, T., Peter, M.*, et al.* (2016). smiFISH and FISH-quant - a flexible single RNA detection approach with super-resolution capability. Nucleic Acids Res *44*, e165.

Tutucci, E., Vera, M., Biswas, J., Garcia, J., Parker, R., and Singer, R.H. (2018). An improved MS2 system for accurate reporting of the mRNA life cycle. Nature methods *15*, 81-89.

Vattem, K.M., and Wek, R.C. (2004). Reinitiation involving upstream ORFs regulates ATF4 mRNA translation in mammalian cells. Proc Natl Acad Sci USA *101*, 11269-11274.